Engineering Geology 220 (2017) 52–64

Contents lists available at ScienceDirect

Engineering Geology

journal homepage: www.elsevier.com/locate/enggeo

Field scale hydraulic conductivity and compressibility of organic clays

Navid H. Jafari [a,*], Timothy D. Stark [b]

[a] Dept. of Civil and Environmental Engineering, Louisiana State University, 3504 Patrick Taylor Hall, Baton Rouge, LA 70803, United States
[b] Dept. of Civil and Environmental Engineering, Univ. of Illinois, 205 N. Mathews Ave., Urbana, IL 61801-2352, United States

ARTICLE INFO

Article history:
Received 3 August 2016
Received in revised form 30 December 2016
Accepted 14 January 2017
Available online 20 January 2017

Keywords:
Hydraulic conductivity
Soil compressibility
Scale effect
Transient seepage
Consolidation
Organics

ABSTRACT

This paper uses the results of an extensive subsurface investigation performed along the Inner Harbor Navigational Canal in New Orleans, Louisiana to identify the scale effect of soil hydraulic conductivity (K) and compressibility (m_v) for geotechnical and geoenvironmental analyses. The magnitude and variability of soil hydraulic conductivity and compressibility parameters were obtained from laboratory 1-D consolidation and permeameter tests, CPTu dissipation tests, field piezometer slug tests, and multiple well pump tests. The geometric means of horizontal hydraulic conductivity (K_h) measured by the laboratory permeameter, slug, and field pump tests are 2.5×10^{-7}, 1.6×10^{-6}, and 1.3×10^{-5} cm/s, respectively. This represents a scale effect of about 50 times when increasing the sample volume tested from the laboratory to field scale. The uncertainty in vertical hydraulic conductivity (K_v), K_h, and m_v values was determined using a coefficient of variation, which ranges from 0.34 to 0.73. While K_h is scale dependent, a comparison of m_v evaluated from field pump and 1-D consolidation tests indicates that sample volume does not significantly impact measured values of m_v, which signifies that laboratory consolidation tests can be used to predict field scale compressibility.

© 2017 Elsevier B.V. All rights reserved.

1. Introduction

Evaluating the field-scale hydraulic conductivity and compressibility of soft organic clays that dominate fluvial-deltaic deposits, e.g., the Mississippi River Delta and Sacramento-San Joaquin River Delta, is important for geotechnical and geoenvironmental analyses, such as, seepage, stability, consolidation, and contaminant transport. In particular, increasing concentration of industry and population can lead to these fluvial-deltaic clays hosting a large number of chemical spills, superfund sites, and waste disposal facilities (Flawn et al., 1970; Taylor, 1993; Hanor, 1993). Because organic clays also overlie coastal aquifer systems, long-term groundwater withdrawals can result in significant consolidation of these aquitards and ultimately manifest as land subsidence at the ground surface. Examples of urban and agricultural regions affected by groundwater-induced subsidence of thick normally consolidated organic layers include the San Jacinto Basin and San Joaquin Valley in California; Houston-Galveston, Texas; and coastal Louisiana. For example, Smith and Kazmann (1978) estimate approximately 0.4 m of local subsidence in Baton Rouge, Louisiana from 1935 to 1976 due to groundwater withdrawal.

In addition, deltas in Louisiana and California are protected against flooding and storm surges with earthen levees and floodwalls. This infrastructure is prone to long-term settlement due to underlying organic soils and areal subsidence, which results in expensive maintenance costs to periodically raise levee and floodwall crest elevations to maintain flood design. For example, Stark and Jafari (2015) show that the floodwall along the eastern side of the Inner Harbor Navigational Canal (IHNC) had settled 0.46 to 0.61 m (1.5 to 2.0 ft) prior to Hurricane Katrina due to areal subsidence. To predict the time-dependent contaminant migration and rate of consolidation of aquitards and levee foundation soils, the underlying soil hydraulic conductivity and compressibility estimated from laboratory or field measurements are necessary to represent the scale effects of larger geologic formations.

Hydraulic conductivity can be scale-dependent, and it is difficult to represent all in situ features, e.g., fissures, organics, bedding planes, sand/silt seams, among others, in a flexible wall permeameter given the small specimen diameter (Tavenas et al., 1983; Chapuis, 1990, 2004, 2012; Benson et al., 1994). Flexible wall permeameters are suited for testing relatively homogeneous natural deposits and engineered soils to assess the influence of effective stress changes. However, a drawback to laboratory testing is the tendency to select the most uniform or clayey samples because they are easier to trim and require less support (Olson and Daniel, 1981). The advantage of in situ testing is the potential for testing a representative volume of soil, with all in situ features, at the in situ stress state. Typical in situ tests can be conducted by driving a device into the ground (driven piezometer, cone penetrometer, and/or self-boring pressuremeter) or by drilling a borehole (standpipe piezometer slug, field pump, and/or borehole packer tests). These tests can directly or indirectly measure the in situ hydraulic conductivity. Slug tests and multiple well pump tests permeate fluid into the surrounding soil (Chapuis, 1998; Chapuis and Chenaf, 2002;

* Corresponding author.
E-mail addresses: njafari@lsu.edu (N.H. Jafari), tstark@illinois.edu (T.D. Stark).

http://dx.doi.org/10.1016/j.enggeo.2017.01.015
0013-7952/© 2017 Elsevier B.V. All rights reserved.

Chapuis et al., 2005), while indirect techniques (cone dissipation test) monitor the dissipation of excess pore-water pressure in the ground after expanding a cavity (Burns and Mayne, 1998).

The test interpretation used in the field assumes that the medium has uniform hydraulic conductivity. However, the subsurface is usually heterogeneous and variable, and may include features, such as fissures, sand/silt laminae, and/or organics. As a larger volume of the subsurface is tested, preferred flow pathways are encountered which leads to varying values of hydraulic conductivity at different scales. Available literature indicates an increase in hydraulic conductivity with specimen volume for geologic materials ranging from clay-rich glacial tills to alluvium to fractured rocks (Rovey and Cherkauer, 1995; Schulze-Makuch et al., 1999; Jones, 1993). Most of these data were obtained by comparing laboratory tests, field slug tests (piezometers and packer tests), and large pumping tests. In general, there is an overall increase in hydraulic conductivity as testing moves from laboratory scale (tested volume is 10^{-5} to 10^{-3} m^3), to borehole test scale (10^{-3} to 10^{1} m^3), and to large field pump test scale (10^{1} m^3 or more) (Ratnam et al., 2005).

Neuzil (1986) describes the many challenges faced to obtain estimates of hydraulic conductivity in low hydraulic conductivity formations, e.g., extrapolating small-scale and short-duration tests to larger scale and durations. As a result, limited data is available on the field-scale hydraulic conductivity and compressibility of organic clay layers. To quantify the scale effects of hydraulic conductivity, this paper uses the results of the field and laboratory testing program performed along the eastern side of the IHNC floodwall in New Orleans, Louisiana. The purpose of this testing program was to obtain estimates of in situ hydraulic conductivity and compressibility for floodwall seepage and stability analyses in organic clay and organic-rich layers that were found intermittently in the thicker marsh clay deposits underlying the IHNC floodwall. Because field pump tests are rarely performed in fine-grained strata, this paper also describes the equipment and analysis procedures of four field pump tests conducted during this study, provides a comparison between field and laboratory hydraulic conductivity and compressibility of organic clays, and discusses the variability of hydraulic conductivity along the IHNC.

2. Characterization of IHNC subsurface

The IHNC is located just west of the Lower Ninth Ward (LNW) in Saint Bernard Parish, Louisiana. The IHNC in Fig. 1 runs essentially north-south with the southern end connecting to the Mississippi River

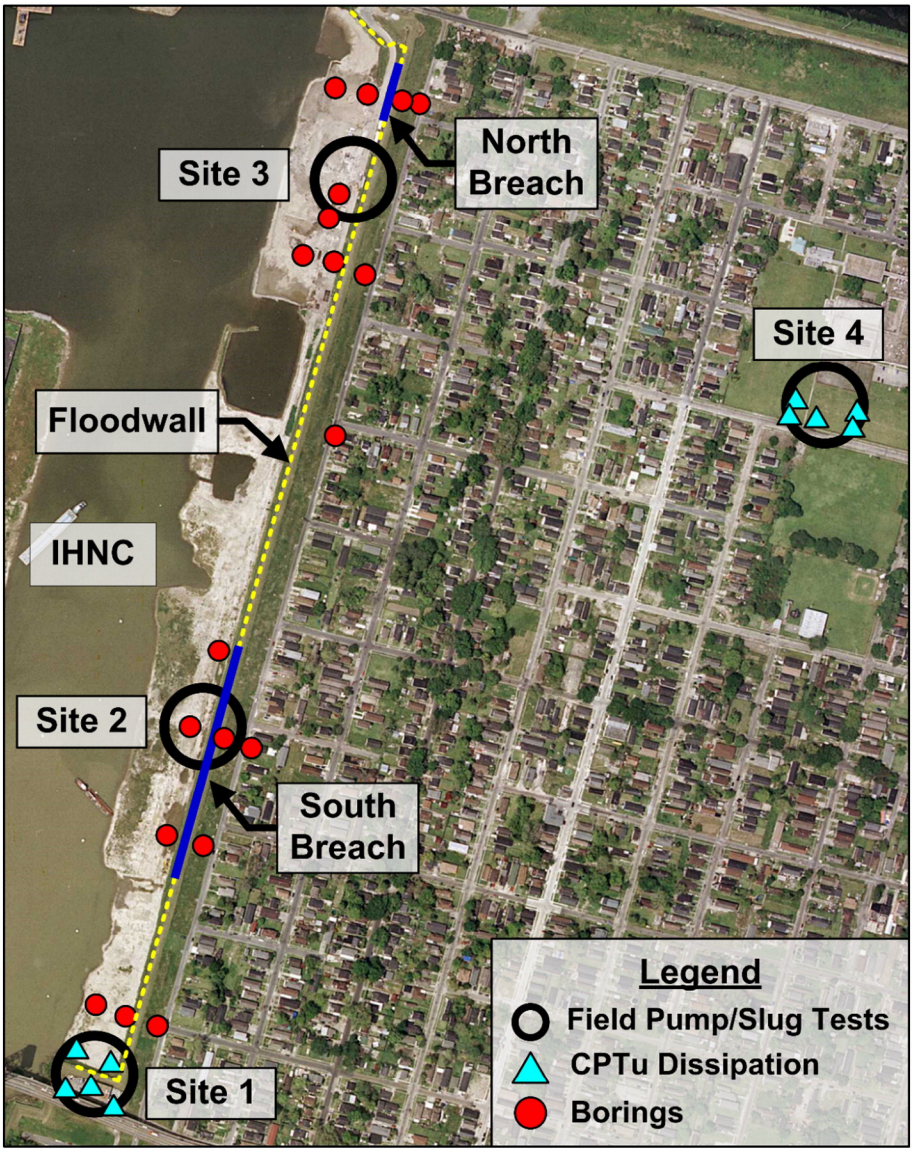

Fig. 1. Overview of IHNC and location of floodwall breaches, field tests, and borings used to obtain high-quality laboratory samples [background image courtesy of Gulf Coast Aerial Mapping (GCAM), with permission].

and the north end connecting with Lake Pontchartrain. During Hurricane Katrina, two failures of the I-floodwall occurred between the Florida Avenue Bridge at the north and the Claiborne Avenue Bridge at the south. A geotechnical subsurface investigation was conducted in 2011 to generate field and laboratory data to better define the soil stratigraphy and quantify the effect of underseepage on floodwall stability (Stark and Jafari, 2015).

This field investigation consists of 40 mud rotary borings with a diameter of 127 mm and 50 piezocone penetration (CPTu) soundings, with approximately equal distribution on the floodside and landside of the I-wall. Some of the floodside investigation locations required a marsh buggy because of IHNC water or soft soils. Otherwise, a typical truck-mounted drill rig was used for both floodside and landside borings. The borings were drilled using the mud-rotary method to increase the removal of cuttings, clean-out of the boring, and reduce the potential for borehole caving. Soil samples were obtained in 1.3 m intervals to the boring completion depths by hydraulically pushing a 127 mm diameter, 1.4 m long thin-walled sample tube using piston sampling techniques (ASTM D1587). Four field pump wells and 48 pump test observation wells were installed to conduct four continuous field pump tests at various locations (Fig. 1) to measure in situ hydraulic conductivity and compressibility of the organic clays underlying the I-wall. In addition to the field investigation and testing, extensive laboratory testing was performed on specimens from the thin-walled sample tubes for soil index properties, hydraulic conductivity, and compressibility. Overall, 74 consolidation and 35 hydraulic conductivity tests were performed on high-quality organic clay specimens to assess the vertical (K_v) and horizontal (K_h) hydraulic conductivity of the clays along and immediately below the sheet pile.

Based on this subsurface investigation, the main soil stratigraphic units below the I-wall are from top to bottom (Fig. 2): (1) levee embankment and fill – compacted organic clays dredged during IHNC construction; (2) upper organic clay – indicative of a swamp deposit with significant fine-grained material as a result of frequent Mississippi River flooding with sediment laden water; (3) lower organic clay – indicative of a marsh deposit with higher organic content than a swamp deposit but still primarily fine-grained material; and (4) interdistributary (ID) clay – a uniform normally consolidated fine-grained clay layer created in a fluvial-deltaic environment.

The levee fill and dredged spoils are comprised of dredged organic and ID clays from creation of the IHNC. The fill material consists of a heterogeneous mixture of gray, soft to stiff lean clay, silt, silty sand, and shell fragments. The levee fill exhibits a natural water content (w_o), liquid limit (LL), and plasticity index (PI) of 43–68%, 73–103%, and 21–76%, respectively (Table 1). The upper and lower organic clays were deposited in swamp and marsh environments, respectively, and are classified as organic clay according to the Unified Soil Classification System (USCS) using ASTM D2216, D2487, D2974, and D4427. These clay layers do not classify as a fibrous peat using ASTM D2974 and D4427, because the organic content (2 to 62%) is less than 75% and a large percentage of gray fine-grained material is present as a result of the frequent flooding and deposition of clay material. The upper and lower organic clays are differentiated by natural water contents below and greater than 100%, respectively. The ID clay consists of gray to dark gray, medium to soft clay with lenses of silty sand and silt and medium lean clay. The ID clay w_o, LL, and PI range from 34–80%, 33–97%, and 16–72%, respectively. Table 1 summarizes the soil classification, saturated unit weight (γ_{sat}), w_o, LL, and PI values of these four soil layers. Dunbar and Britsch (2008) provide additional details on site geology and formation of these soil stratigraphic units along the IHNC.

Table 1
Engineering index properties for soils along eastern side of IHNC between Florida and Claiborne Avenues.

Soil type and classification		γ_{sat} (kN/m^3)	w_o (%)	LL (%)	PI (%)
Levee fill and Dredged spoils	CH	16.3	43–68	73–103	21–76
Upper organic clay	OH	11.8–16.7	42–112	69	46
Lower organic clay	OH	9.9–13.7	116–451	139	81
Interdistributary (ID) clay	CH	18.0	34–80	33–97	16–72

3. Laboratory and in situ test methodology

3.1. One-dimensional consolidation tests

The hydraulic conductivity and compressibility characteristics (Fig. 1 shows sampling locations) of the organic clays were measured using one-dimensional (1-D) incremental and constant rate of strain (CRS) consolidation tests. The incremental consolidation tests were performed on 64 mm (2.5 in.) and 102 mm (4 in.) diameter specimens, and the consolidation load was applied in 8 stages for 24 h at a load increment of unity, which resulted in a final effective stress was 16,000 psf (ASTM D2435). The value of K_v was inferred from the coefficient of consolidation (c_v) and coefficient of volume compressibility (m_v) at the field effective vertical stress using Eq. (1). In particular, the value of c_v was computed using the average of the square root (Taylor, 1942) and log time methods (Casagrande and Fadum, 1940), and m_v was estimated from the end-of-primary vertical strain and effective stress relationship.

$$K_v = c_v \gamma_w m_v \tag{1}$$

The CRS consolidation tests were performed on 64 mm (2.5 in.) diameter specimens per ASTM D4186 (ASTM, 2015a,b), with the

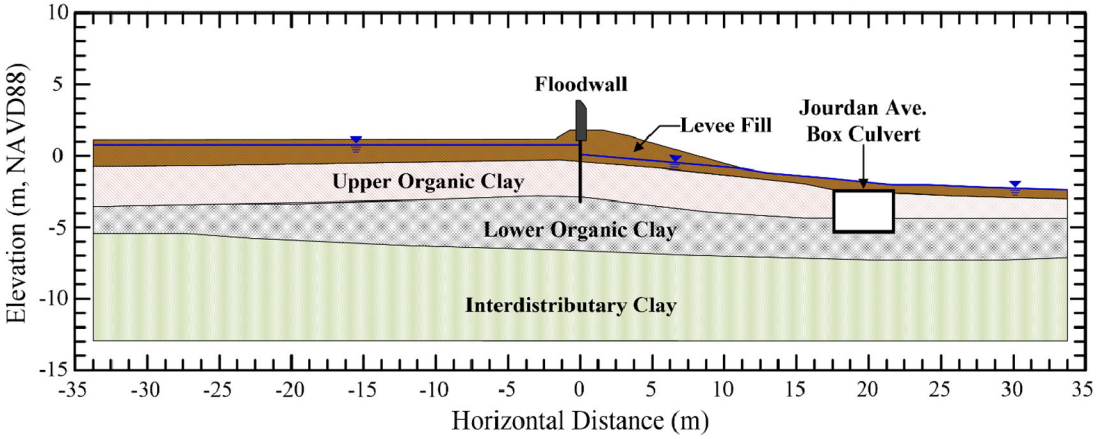

Fig. 2. Generalized IHNC I-wall cross-section that shows sheet pile supported floodwall, initial phreatic surface, and a landside backfilled excavation.

hydraulic conductivity estimated from Eq. (2) for a given specific time n. For both tests, the K_v is evaluated at the in situ overburden stress.

$$K_v = \frac{\dot{\varepsilon}_v \cdot H_n \cdot H_o \cdot \gamma_w}{2 \cdot \Delta u_{m,n}} \times \frac{1}{10,000} \quad (2)$$

where $\dot{\varepsilon}_v$ is the strain rate, H_n is the specimen height (cm) at time n, H_o is the initial specimen height (cm), $\Delta u_{m,n}$ is the base excess pressure which is the difference of the measured base pressure and chamber pressure, and K_v is in m/s. Similar to the 1-D incremental loading test, the value of m_v was estimated from the end-of-primary vertical strain-effective stress relationship.

3.2. Flexible wall permeameter tests

Flexible wall permeameter tests (ASTM D5084) were conducted to evaluate K_v, K_h, and anisotropy ratio (K_h/K_v) of the organic clay layers. Fig. 1 shows locations of the mud-rotary borings used to obtain high quality samples used in the permeameter testing. In addition to conventional 71 mm (2.8 in.) and 102 mm (4.0 in.) diameter permeameter tests, 127 mm (5 in.) diameter permeameters were constructed to test the largest possible test specimen diameter, i.e., diameter of sampling tube, and evaluate the effect of specimen diameter on hydraulic conductivity. To determine K_h, a 127 mm (5 in.) specimen was positioned horizontally and trimmed to obtain a specimen perpendicular to the vertical direction of the original sample. The test specimens were isotropically consolidated to the field effective vertical stress, where in situ hydraulic conductivity was measured. The permeant fluid was either site water or de-aired water, with a hydraulic gradient of five for all permeameter tests.

3.3. Cone penetrometer dissipation tests

Fourteen CPTu dissipation tests were conducted within a 5 m radius of field pump test Sites 1 and 4 (Fig. 1 for locations). A cone dissipation test was performed by advancing a 10 cm^2 cone-tip to the bottom of the lower organic clay. After advancement of the cone to a desired depth and the penetration force was released from the cone rods, the dissipation of the excess pore-water pressure induced during penetration was recorded until an equilibrium condition was achieved or 50% of the initial excess pore-water pressure dissipated. In normally consolidated soils, the (t_{50}) time at 50% dissipation (t_{50}) can be used to determine the value of K_h. Schmertmann (1978), Parez and Fauriel (1988), and Robertson et al. (1992) suggest methods to estimate K_h using the t_{50} value. In particular, the empirical method proposed by Parez and Fauriel (1988) based on the measured t_{50} (seconds) from the dissipation curve was used to estimate K_h (cm/s) using Eq. (3).

$$K_h \approx \frac{1}{(251 \cdot t_{50})^{1.25}} \quad (3)$$

4. Field slug and pump tests

4.1. Well construction and testing

Field pump tests were conducted at four locations, with Sites 1 through 3 located along the proximity of the IHNC floodwall and Site 4 located in the LNW (Fig. 1). Because the test methodology and data analysis are the same for all four sites, only detailed overview of Site 1 is provided herein, with the results from all field pump tests are presented subsequently. Site 1 is located at the south end of the IHNC near the Claiborne Ave Bridge. Fig. 3(a) shows the pumping well and landside monitoring wells, while Fig. 3(b) shows the floodside monitoring wells which served as baseline wells to determine the regional groundwater flow regime and detect if underseepage occurred under the sheet pile wall due to pumping. Fig. 3(c) shows a plan view of the pumping well in relation to the floodwall and monitoring wells. The landside monitoring wells are within 3 m of the pumping well, and the floodside monitoring wells are located within a radius of about 12 m from the pumping well.

The pumping wells were installed in accordance with ASTM D5092 using a 15.2 cm diameter rotary wash boring with water as the drilling fluid. Each pumping well was constructed using a 51 mm diameter by 1.5 m long PVC casing and 0.9 m screened section with a slot size of 0.254 mm. Usually 150 mm of sand was placed below and above the screened section as well as in the screened section. The tip of the screened interval screen was placed at or near the bottom of the Lower Organic Clay layer because it is below the tip of the sheet pile cut-off wall (Fig. 2), which was key to determining if underseepage contributed to the floodwall failures. The depth and thickness of the Lower Organic Clay layer were determined from the subsurface investigation, which was identified when the natural moisture content increased above 100% in the organic clay deposits. Fig. 4 shows the relevant soil profile, screen location, sand pack, and other installation parameters for the pumping well PW-1 at Site 1.

For each site, six monitoring well (MW) locations were selected and at each location two monitoring wells in close proximity to each other were screened at shallow (S) and deep (D) depths, as shown in the plan view in Fig. 3(c). The monitoring wells depicted in Fig. 5 were constructed using 60 mm outside diameter pre-pack well screen. The pre-pack well screen consists of 38 cm Schedule 40 PVC with a 0.254 mm slot size. The inner PVC well screen was 0.6 m in length with a flush plug on one end and ASTM F480 flush thread on the other. The outer component of the screen is stainless steel wire mesh with a pore size of 0.28 mm and was packed with 20/40 environmental grade sand. In general, 15.2 cm of sand was inserted above the screen, resulting in a collection zone of about 0.75 m.

Each monitoring well location consists of two pre-packed screens in adjacent holes. The deeper pre-pack screen was placed in the Lower Organic Clay layer, e.g., MW-5D in Fig. 5, as determined by soil sampling and cone penetrometer soundings at each pump test location. The upper screen section was placed in the upper organic clay layer (e.g., MW-5S). Both pre-pack well screens were placed using direct push in accordance with ASTM D6724. The efficacy of well development was evaluated by conducting a slug test in each well following installation in accordance with either ASTM D4044 or ASTM D7242. Following the initial slug test, the pumping and monitoring wells were developed and allowed to recover within 90% of the displaced static level measured prior to the first slug test. A second slug test was performed and compared to the first slug test to evaluate efficacy of well development. The well was considered adequately developed if the calculated hydraulic conductivity value of the pumping well from the second slug test was within 30% of the first test. This test procedure was repeated with additional slug test cycles to verify that the control and observation wells were adequately developed before starting the field pump test.

Water levels in pumping and monitoring wells were initially measured manually with a test-site designated electronic water level indicator. Each pumping and monitoring well was later equipped with a pressure transducer to monitor water levels prior to, during, and after the pumping tests. Pressure transducers were calibrated in accordance with the manufacturer instructions and the calibration was field-verified in accordance with ASTM D4050. The water level in the IHNC was also monitored at a point located within one mile of all pumping test sites. Barometric pressure was also monitored using a pressure transducer. For each test site, the water levels were monitored every 15 min in the pump and monitoring wells for a period of at least 48 h prior to the start of the pumping test.

Sampling and testing at the IHNC characterized the subsurface stratigraphy as organic clay deposits with some organic material (roots, stems, and pieces of wood), which overlain by fine-grained soils. As a result, the organic clay layers have limited ability to yield appreciable

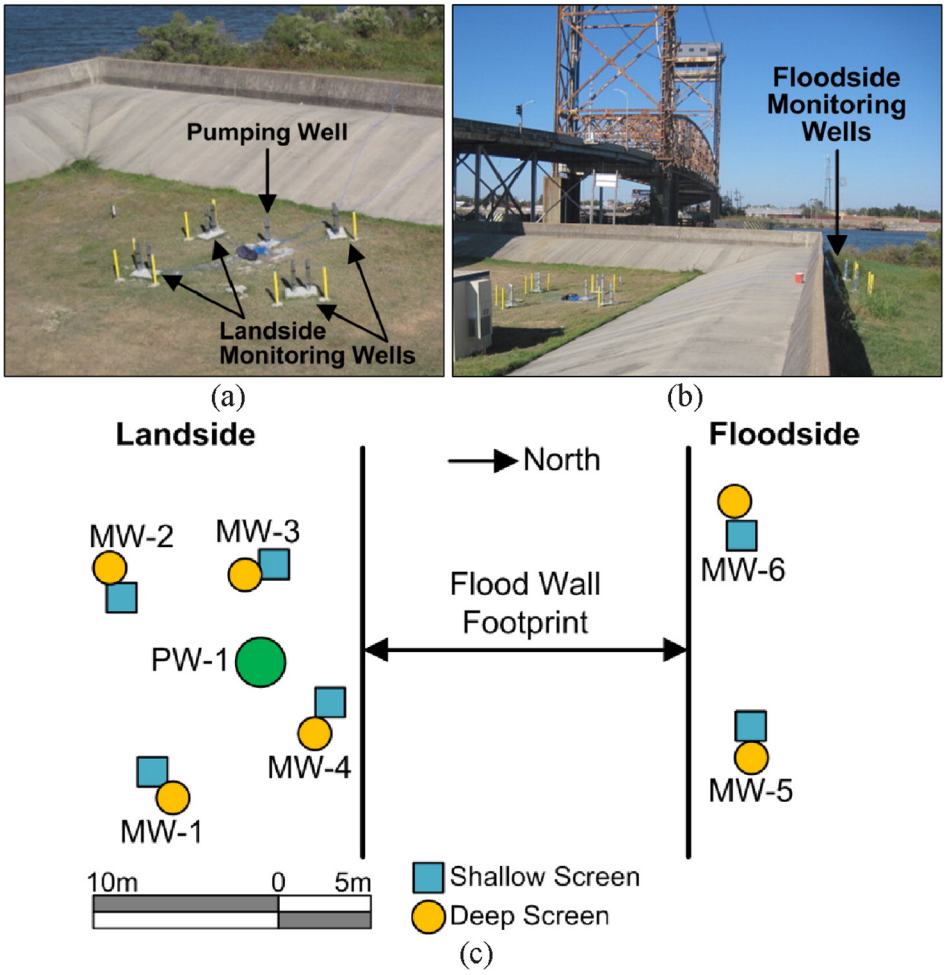

Fig. 3. Field Pump Test at Site 1: (a) landside pumping and monitoring wells with the floodwall in the background; (b) floodside monitoring wells; and (c) plan view of the field pump test layout.

volumes of water to a pumping well. Because the field pump test methods were developed for granular soils, many of the ASTM methods, e.g., ASTM D4050, had limited applicability to the pumping tests in the Lower Organic Clay along the IHNC. To be in conformance with ASTM methods, the constant head and traditional constant rate pumping tests were employed at the IHNC. In particular, the pumping tests for Sites 1 and 4 were conducted using traditional constant rate test methods, whereas Sites 2 and 3 used the constant head test methods. In the constant head pumping test, water was discharged from the pumping well to maintain a constant water level (constant head) in the pumping well. The pumping tests required the use of a peristaltic pump using a flow rate of 100 ml/min or less to maintain a constant level in the pumping well. The flow rate was calculated by measuring the volume of water discharged to a graduated cylinder or other measuring device over a 5 minute interval. In contrast, the traditional constant rate test method involves setting a constant flow rate and monitoring the change in pumping well water level with time.

4.2. External influences on in situ hydraulic testing

Kruseman and de Ridder (1990) recommend analyzing the hydraulic response induced by the pumping tests to determine if external influences are affecting the pump tests. External influences that can be encountered during the testing program include rainfall, storm water pumping from the storm water removal system, and tidal fluctuations. Sufficient antecedent data is also needed to properly identify and quantify the outside influences. Rainfall was measured with an onsite gauge and supplemented with rainfall data from a proximal NOAA rainfall gauge for periods when site data was not available. During the field testing, Tropical Storm Lee was responsible for the rainfall total of 27.6 cm from 2 to 4 September 2011. A direct response to and lingering replenishment of groundwater from the rainfall events were measured in a majority of the testing locations. Stormwater drainage structures are also located proximal to the testing locations. A pumping station (located north of Site 3 and the North Breach but out of view in Fig. 1) pumped during extended periods of no rainfall, resulting in removal of groundwater. Canal water elevation data was obtained from a stilling well positioned in the IHNC adjacent to Site 1. The stilling well data was measured from 13 September 2011 to 3 November 2011. Tidal data from a nearby NOAA tidal gauge (Shell Beach gauge [NOAA station 8761305]) was acquired to confirm the IHNC tidal response. The data indicates a correlation between (also indicating tidal lag) the IHNC tidal level and the Shell Beach gauge which is located approximately 37.4 km (22 miles) from the testing site. A tidal response is noted in several of the testing locations throughout the testing program as well as the IHNC and Shell Beach tidal responses used in analyzing the pumping tests.

4.3. Model input parameters

The field slug and multiple well tests were analyzed in accordance with Kruseman and de Ridder (1990) and ASTM D4050, and utilizing the pump and slug tests analysis software AQTESOLV (Duffield, 2007). To analyze data from slug tests and pumping tests with AQTESOLV,

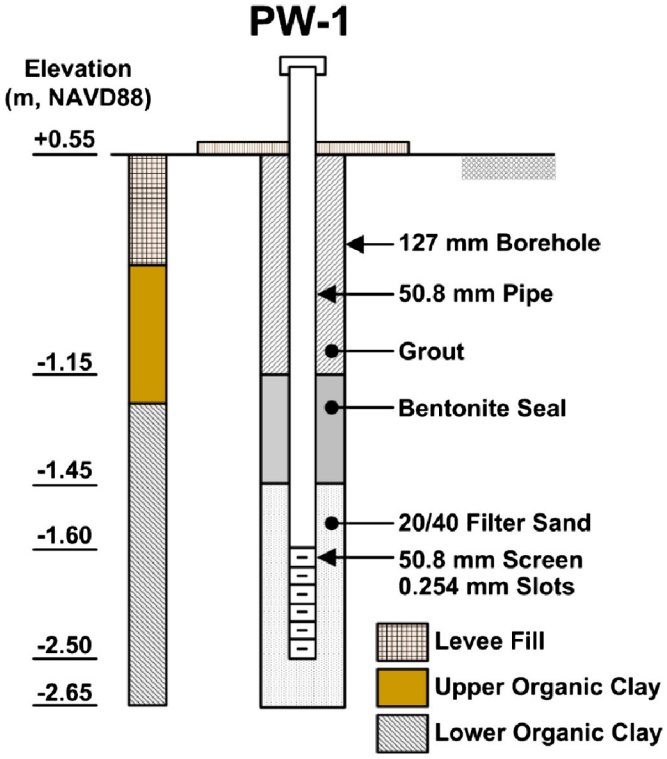

Fig. 4. Cross-section and soil profile at PW-1 for Site 1 Pump Test (elevation not to scale).

the hydraulic parameters, test well dimensions, and subsurface dimensions are required. A summary of the AQTESOLV input parameters used in the hydraulic data analysis for each site is presented in the Supplemental Data Tables S1 through S4. Several of the input parameters were obtained from the well construction logs. These input parameters include the observed initial displacement (H_o); static water column height (H); depth to top of well to groundwater surface (d); inside radius of well casing (r_c); radius of well (r_w); and well skin radius (r_{sk}). The input parameters which require interpretation and the rationale behind the parameter selection include length of well screen (L); aquifer thickness (b); and anisotropy ratio (K_h/K_v). The aquifer thickness is based on the soil profile documented in the nearest boring(s) to each testing site, with the target testing interval being the Lower Organic Clay layer. If the filter pack of the testing well intercepted this layer by at least 0.3 m, the aquifer thickness was assigned the thickness of the Upper or Lower Organic Clay layer observed in the nearest soil boring. Otherwise, the thickness of the filter pack was used as the aquifer thickness. Because pumping test analyses require a single aquifer thickness condition, the aquifer thickness of the monitoring wells was averaged. The horizontal to vertical anisotropy ratio (K_h/K_v) of soft clays caused by the orientation of clay minerals in unconsolidated sediments is usually less than 3 (Terzaghi et al., 1996). However, Freeze and Cherry (1979) suggest it is not uncommon for layered heterogeneity to lead to regional anisotropy ratios of 100 or even larger. Based upon the clay-rich nature of the sediments encountered at the testing site, a K_h/K_v of 10 was initially selected.

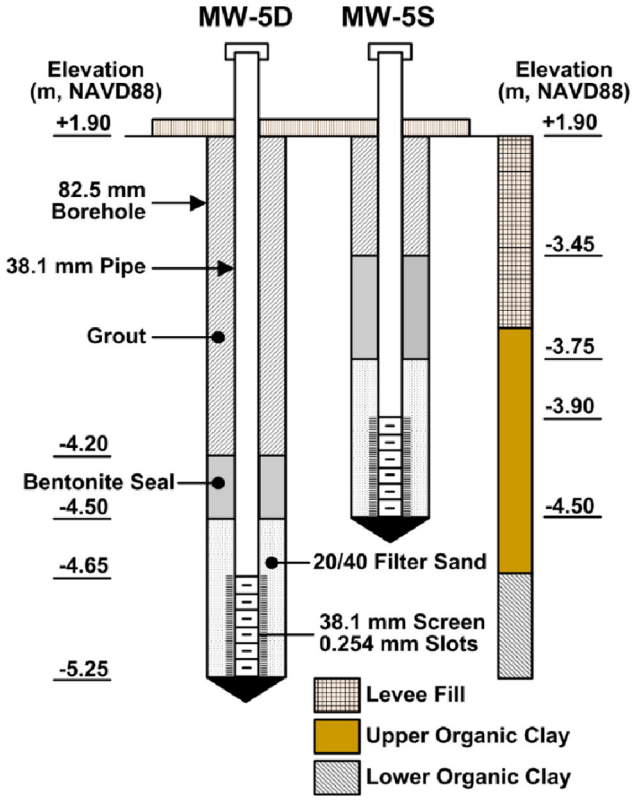

Fig. 5. Cross-section and soil profile of MW-5S and MW-5D at Site 1 (elevation not to scale).

4.4. Slug test analysis

The field slug testing method consists of rapidly raising or lowering the level of groundwater in a well and measuring the time the water requires to regain the initial level. From the water level data and dimensions of the piezometer, the in situ K_h was estimated for the portion of the deposits that are contributing water to the screened interval of the piezometer. The analysis was performed using the aquifer testing analysis software AQTESOLV with the input parameters summarized in Tables S1 through S4. The analytical methods employed for estimating K_h are the unconfined Hvorslev (1951) and the unconfined Bouwer and Rice (1976) methods. Bouwer and Rice (1976) developed an empirical relationship describing the water-level response in an unconfined aquifer due to the instantaneous injection or withdrawal of water from a well. The assumptions for Bouwer and Rice (1976) and Hvorslev (1951) include the aquifer has infinite areal extent, is homogenous and uniform in thickness, is fully or partially penetrating; and, the flow to the well is quasi-steady-state, i.e., the model ignores elastic storage of the aquifer. The confined Hvorslev (1951) solution for confined solutions can approximate unconfined conditions when the well screen is below the groundwater surface.

Fig. 6 shows the time-dependent drawdown curves of slug tests for monitoring wells located on the landside (MW-1D) and floodside (MW-6D) of the floodwall. The linear trend line in Fig. 6 represents the solutions for both analytical methods. Both monitoring wells show that the Hvorslev and Bouwer-Rice methods yield similar K_h values. For example, MW-1D and MW-6D indicate the average Lower Organic Clay layer K_h layer is about 4.5×10^{-6} cm/s and 1.5×10^{-6} cm/s, respectively. Up to five slug tests were performed on each pumping and monitoring well in at each pump test site along the IHNC. The initial slug test was performed prior to well development and the subsequent tests were performed following varying stages of development. The results from both analytical methods were used at each well to determine a geometric mean. As a result, a value of K_h is provided for each pumping and monitoring well involved in the four field pump tests, with the range of K_h and geometric mean provided in Table 2.

4.5. Pump test analysis

The estimation of in situ K_h from the field pump tests was performed using the software AQTESOLV, with the input parameters summarized in Tables S1 and S4. The AQTESOLV solutions for multiple pump tests provide an estimate of transmissivity, so the value of K_h is determined

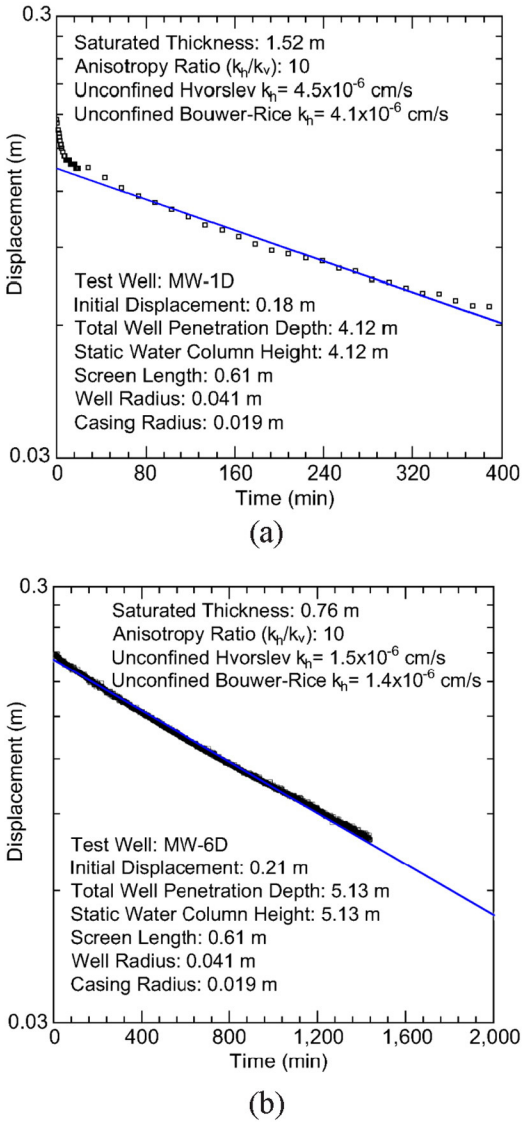

Fig. 6. Site 1 field slug test results for: (a) MW-1D and (b) MW-6D

by dividing transmissivity by the aquifer thickness. A total of four pumping tests were conducted using the traditional constant rate test method at Sites 1 and 4 and the constant head test method at Sites 2 and 3, which provided an opportunity to measure in situ K_h from drawdown and recovery periods. The drawdown analyses for all four sites used the unconfined aquifer solutions from Theis (1935) and Cooper and Jacob (1946). The recovery analysis at Sites 1 and 4 applied unconfined aquifer solutions from Neuman (1974) and Tartakovsky and Neuman (2007), whereas Sites 2 and 3 employed leaky confined aquifer solutions of Hantush (1959) and Moench (1985). Site 1 is used to illustrate the analysis procedure for estimating in situ K_h, which was applied to the remaining three sites. Site 1 involved two traditional constant rate tests, and K_h was estimated from drawdown and recovery periods. The first test continued for four days and the flow rate initially ranged from 17 to 41 ml/min before equilibrating at 20 ml/min after about 10 min into the pumping period. During the four day test, a total of 114 l was removed from the pumping well. Fig. 7 shows the hydrograph of the shallow test wells at Site 1. Drawdown was observed in shallow monitoring wells MW-1, MW-2, MW-3, and MW-4. Although the floodside monitoring wells in Fig. 7 exhibit a steady decrease in water elevations during the drawdown period, this behavior corresponds to an external regional downward drift in the surrounding area groundwater levels. To remove the regional drift from the drawdown data, the floodside monitoring wells were corrected using the regional groundwater level trend analysis to evaluate baseline conditions along the IHNC. The equations used to correct the floodside wells were then applied to the monitoring well data on the landside to. By correcting for external influences, negligible water elevation decrease occurred in the floodside monitoring wells during the pumping period, i.e., negligible underseepage under the sheet pile of the floodwall.

After the external influences were accounted for, the in situ K_h during drawdown was estimated using the unconfined Theis (1935) and Cooper and Jacob (1946) solutions. Both solutions are derived for unsteady flow to a fully penetrating well in a confined aquifer. The solutions also assume a line source for the pumped well, thus neglecting wellbore storage. Because Theis (1935) and Cooper and Jacob (1946) solutions are developed for confined aquifers, the drawdown data is corrected for displacement before they were applied to unconfined aquifers. The corrected displacement is plotted against log-scale time to solve the Theis (1935) and Cooper and Jacob (1946) solutions, as shown in Fig. 8. The Cooper and Jacob (1946) method analyzes pump tests based on a straight-line approximation, while the Theis (1935) uses an exponential function to model the time-dependent behavior. Typically, the Cooper and Jacob (1946) linear curve matching (Fig. 8) is performed first to obtain an estimate of transmissivity before solving the Theis (1935) equation. In Fig. 8, the transmissivity of MW-3S is about 1.3×10^{-2} cm^2/s and 9.8×10^{-3} cm^2/s for Cooper and Jacob (1946) and Theis (1935) solutions, respectively. Given a saturated aquifer thickness of 0.91 m, the corresponding in situ K_h for Cooper and Jacob (1946) and Theis (1935) solutions is 1.4×10^{-4} cm/s and 1.1×10^{-4} cm/s, which shows that both methods are in good agreement.

After completing the drawdown period and the pumping was stopped, the water level in pumping well PW-1 was allowed to recover. The recovery analysis was performed using the unconfined Neuman (1974) and Tartakovsky and Neuman (2007) solutions. Similar to the drawdown data, a correction for regional drift based on the floodside monitoring wells was applied to PW-1. Fig. 9 shows the recovery levels in PW-1 in terms of Agarwal (1980) equivalent time. The Agarwal (1980) method uses a transformation of the time scale to allow the use of standard drawdown solutions, e.g., Theis, Cooper and Jacob, and Neuman, for matching recovery data. The recovery transmissivity of PW-1 is about 4.0×10^{-4} cm^2/s for Tartakovsky and Neuman (2007) and Neuman (1974) solutions. Given a saturated aquifer thickness of 1.07 m at PW-1, the corresponding in situ K_h for both solutions is about 3.7×10^{-6} cm/s. Table 2 summarizes the drawdown and recovery in situ K_h obtained from each site.

Table 2
Summary of K_h statistics measured from laboratory permeameter tests, field slug tests, in situ CPTu, and field pump field tests, and in situ CPTu.

IHNC	Permeameter $K_h \times 10^{-6}$ (cm/s)				Field Slug Test $K_h \times 10^{-6}$ (cm/s)				Field Pump Test $K_h \times 10^{-6}$ (cm/s)			CPTu $K_h \times 10^{-6}$ (cm/s)			
Site	n	Range	Mean	COV	n	Range	Mean	COV	n	Drawdown	Recovery	n	Range	Mean	COV
1	3	0.1–0.3	0.17	0.22	12	0.21–5.2	1.2	0.48	4	30	4	8	0.36–25	2.9	0.81
2	2	0.06–0.49	0.21	0.37	13	0.97–5.8	1.8	0.25	3	50	4	–	–	–	–
3	16	0.05–3.1	0.34	0.56	13	0.73–4.8	1.8	0.27	2	8	1	–	–	–	–
4	–	–	–	–	11	2.9–390	22	0.39	2	–	100	17	0.56–100	6.6	0.75

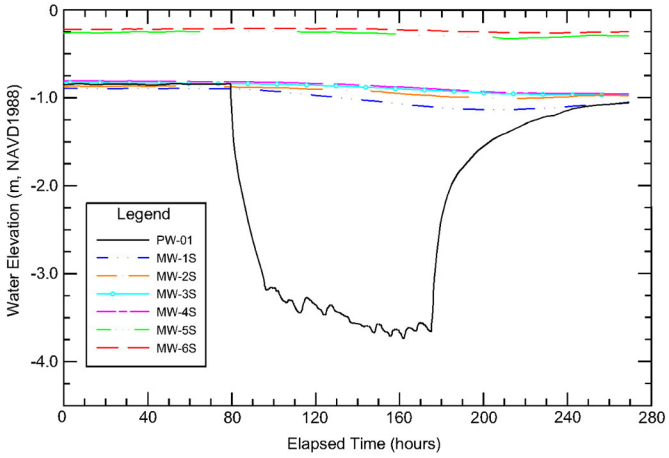

Fig. 7. Time history of water levels of shallow wells during Field Pump Test 1 at Site 1.

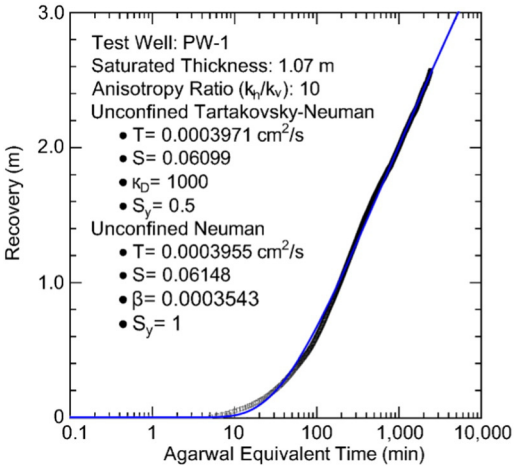

Fig. 9. Site 1 recovery curve showing curve matching trend for Neuman (1974) and Tartakovsky and Neuman (2007) unconfined aquifer solutions.

5. Laboratory and field results

The geometric mean for each test method is shown in Table 2 and was evaluated to obtain a representative value for each test. Table 2 also lists the range and coefficient of variation (COV) of K_h for each test method with the field pump tests reporting single values for drawdown and recovery. To compare the various hydraulic conductivity testing, Fig. 10 shows the data values for each site. For example, Fig. 10(a) shows Sites 1 to 3 permeameter results obtained for sample diameters of 71, 102, and 127 mm. The geometric means for each site occur in the narrow range of 1.7×10^{-7} to 3.4×10^{-7} cm/s. The majority of permeameter tests were performed at Site 3 compared to Sites 1 and 2 because this area is located near the North Floodwall Breach (Fig. 1), which occurred during Hurricane Katrina in 2005. This greater number of tests at Site 3 shows the variability of K_h in the organic clays, e.g., the lower and upper limit of K_h is 5×10^{-8} and 3×10^{-6} cm/s, respectively.

While the geometric mean of K_h from the field slug tests show agreement between Sites 1 to 3 (~1.5×10^{-6} cm/s), the Site 4 values in Fig 10(b) are about a magnitude higher (2.2×10^{-5} cm/s). This difference is attributed to the change in geology over the 0.8 km distance from the floodwall to Site 4 in the LNW. In particular, the borings at Site 4 found predominantly undecomposed vegetation and wood, which is in contrast to the soft, grey clays intermixed with roots, stems, and small pieces of wood observed at Sites 1 through 3 along the floodwall (Fig. 2 soil profile). This decomposing vegetation was the reason laboratory permeameter tests were not performed at Site 4. Fig. 10(b) also shows the slug tests at Site 4 were performed at a shallower depth, which results in a higher void ratio and measured values of K_h than the organic clays found at Sites 1 to 3. The pump test data in Fig. 10(c) combine drawdown and recovery tests to obtain a range of K_h. Sites 1 and 2 report a K_h of ~2×10^{-5} cm/s while the K_h mean at Site 4 (~7.3×10^{-5} cm/s) is slightly higher because of the undecomposed organics.

The Site 3 field pump test is an order of magnitude lower (2.8×10^{-6} cm/s) than the pump tests at Sites 1 and 2, which is reasonable considering the volume of water pumped from Site 3 is about four times less. The CPTu dissipation tests in Fig. 10(d) were performed at Sites 1 and 4. Both sites show a significant range of predicted K_h. For example, the Site 1 K_h values range from 3.6×10^{-7} to 2.5×10^{-5} cm/s with a geometric mean of 2.9×10^{-6} cm/s.

To determine the variability between Sites 1 through 4, an analysis of variance (*ANOVA*) was performed on the field slug test K_h values, where the null hypothesis (H_o) assumed the geometric means for each site are equal. For $\alpha < 0.05$, the *F*-statistic was less than the *F*-critical ($22.36 < 2.81$), so the H_o was rejected. In other words, Sites 1 to 4 geometric means are not statistically equal. To identify the site causing the H_o rejection, a two-tail *t*-statistic hypothesis test was performed comparing the geometric mean for two sites. A single-tail *F*-test was first performed to test if the variances of the two populations were equal or unequal (required for the *t*-statistic test), where the H_o in the single-tail *F*-test assumes the variances are equal. Using Sites 1 and 2 sample data as an example, the *F*-value is greater than the *F*-critical ($3.31 > 2.69$). Thus, the H_o was rejected and the variances are unequal. Then, the *t*-statistic test with unequal variances is performed assuming the geometric means at Sites 1 and 2 are equal. In this case, the *t*-statistic was greater than the two-tail *t*-critical value ($-1.11 > -2.09$), so the value of H_o was accepted and the geometric mean of K_h for Sites 1 and 2 are statistically equal. These steps were repeated for each combination of sites. Based on the *t*-statistic hypothesis tests, Sites 1 through 3 resulted in an accepted H_o, indicating that the K_h geometric means are statistically equal. In contrast, all hypothesis tests with Site 4 (Sites 1 and 4; Sites 2 and 4; Sites 3 and 4) resulted in a rejected H_o, suggesting that the Site 4 K_h from the slug test was statistically different from the geometric means measured from Sites 1 through 3. An *ANOVA* hypothesis test performed on only Sites 1 through 3 resulted in an accepted H_o (*F*-value < *F*-critical), which further validates that Site 4 was the cause of variability in the first *ANOVA* test. In summary, Fig. 10 shows the variability in K_h measured for Sites 1 through 3, i.e., along the IHNC floodwall, is small while Site 4 is higher because of the change in soil type from organic clay to decomposing vegetation in the LNW.

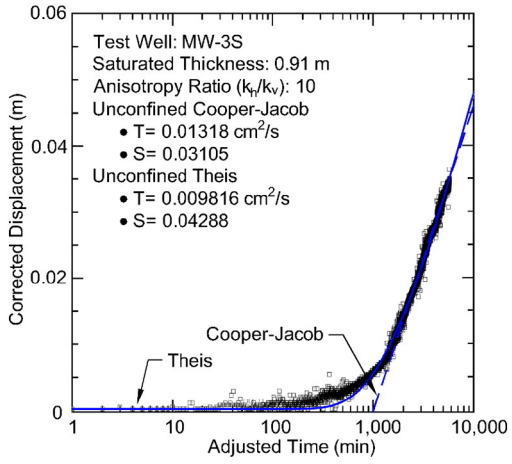

Fig. 8. Site 1 MW-3S corrected drawdown curve showing Theis (1935) and Cooper and Jacob (1946) unconfined aquifer solutions

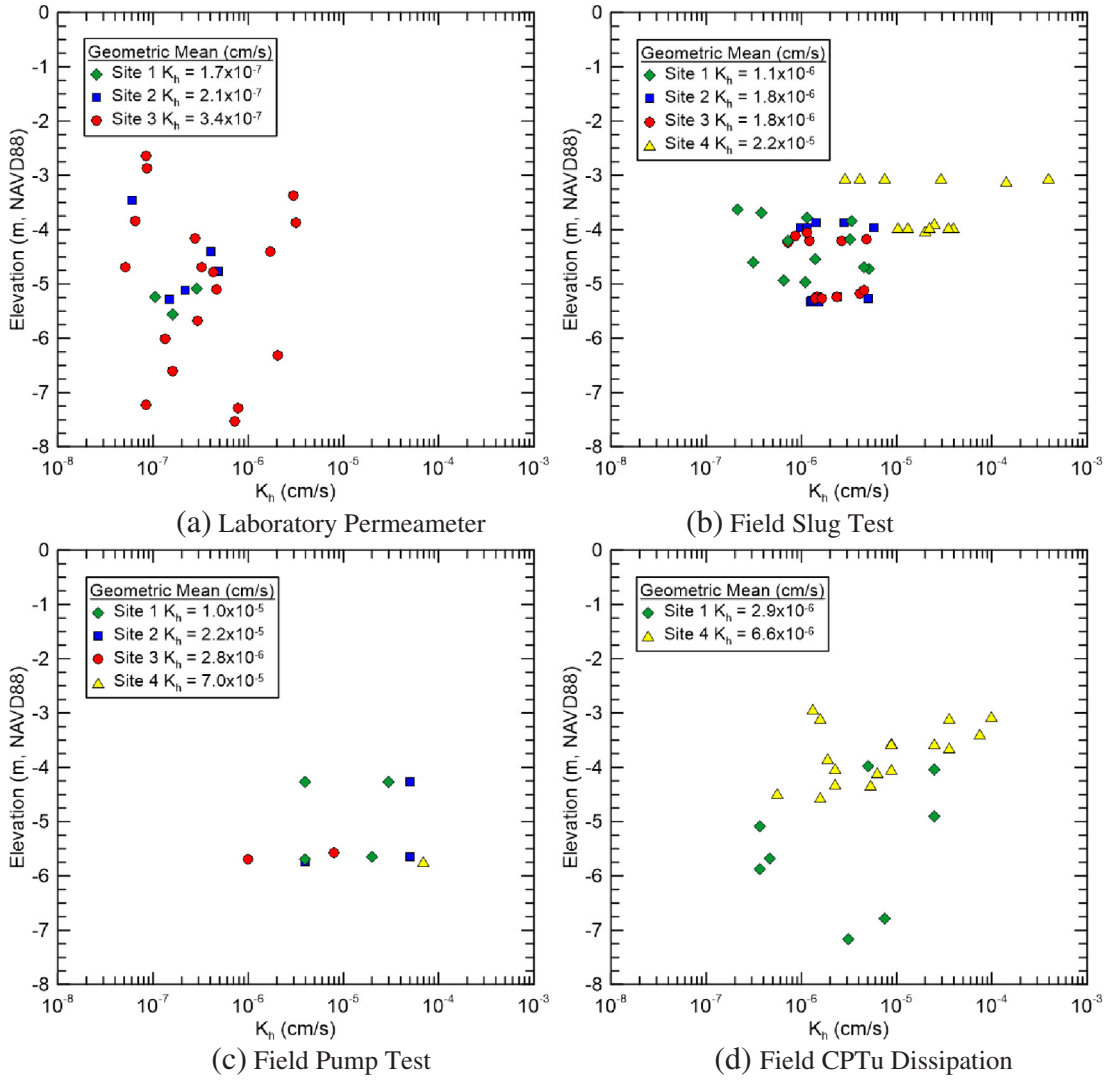

Fig. 10. Summary of K_h results from: (a) Laboratory Permeameter, (b) Field Slug, (c) Field Pump, and (d) CPTu Dissipation Tests.

5.1. Scale effect of K_h

With the data above, the relation of K_h to specimen size can be examined by the distance the water travels during a test, radius of influence, and/or volume of material tested (Rovey and Cherkauer, 1995; Bradbury and Muldoon, 1990). For example, the flow distance of a slug test, i.e., the dimension parallel to flow, is generally only several centimeters into the soil but the procedure is testing several meters of material transverse to flow (along the screen). While the flow distance through a permeameter is also several centimeters, the transverse radius is only in the centimeter range. This distance-parallel-to-flow approach projects both tests on the same scale. With a volume of tested material as the scale measure, these two types of tests are separated by orders of magnitude. As a result, Schulze-Makuch et al. (1999) recommend using the volume of test material as the scale measure. The volume of material tested for permeameters is equal to the volume of the specimen. The field slug and pump test volumes are estimated by the ratio of volume of water extracted or pumped, respectively, to the effective porosity of the soil (n_e), i.e., the porosity available for fluid flow (Peyton et al., 1986; Fetter, 1988). Because water is governed by capillary, gravitational, and molecular forces, the effective porosity is defined as the part of the pore volume where the water can flow. Peyton et al. (1986) define the effective porosity as the difference between total porosity (n_t) and the residual volumetric water content (θ_r). The effective porosity can be determined in the field (tracer study) or in the laboratory, e.g., soil column drainage studies and nuclear magnetic resonance. McWhorter and Sunada (1977) suggest n_e values of 0.01 to 0.18 for clays, with an average of 0.06. Because of the lack of site specific testing, the average n_e value of 0.06 was selected to determine the volume of material tested for the field slug and pump tests. The volume of pumped water was measured using a bailer and flowmeter for the slug and pump tests, respectively.

Fig. 11 shows the effect of increasing volume of material tested at each site. The volume of samples tested in the permeameters is about 3×10^{-4} m^3, and the volumes increased to about 2×10^{-2} m^3 for field slug tests and greater than 1 m^3 for the field pump tests. The geometric means of the permeameter, slug, and pump tests in Fig. 11(a) are 1.7×10^{-7}, 1.1×10^{-6}, and 1×10^{-5} cm/s, respectively. Compared to the Site 1 pump test, the permeameter and slug tests underestimate the organic clay K_h by a factor of 60 and 9, respectively. In Fig. 11(b), Site 2 permeameter and slug tests underestimate the organic clay K_h by a factor of 105 and 12, respectively. A comparison of permeameter and slug tests in Fig. 11(c) suggests that the geometric mean of permeameter tests is lower but the scale effect can be reduced if the number of tests is increased, thereby increasing the likelihood of capturing the heterogeneity of organic clays with laboratory permeameter tests.

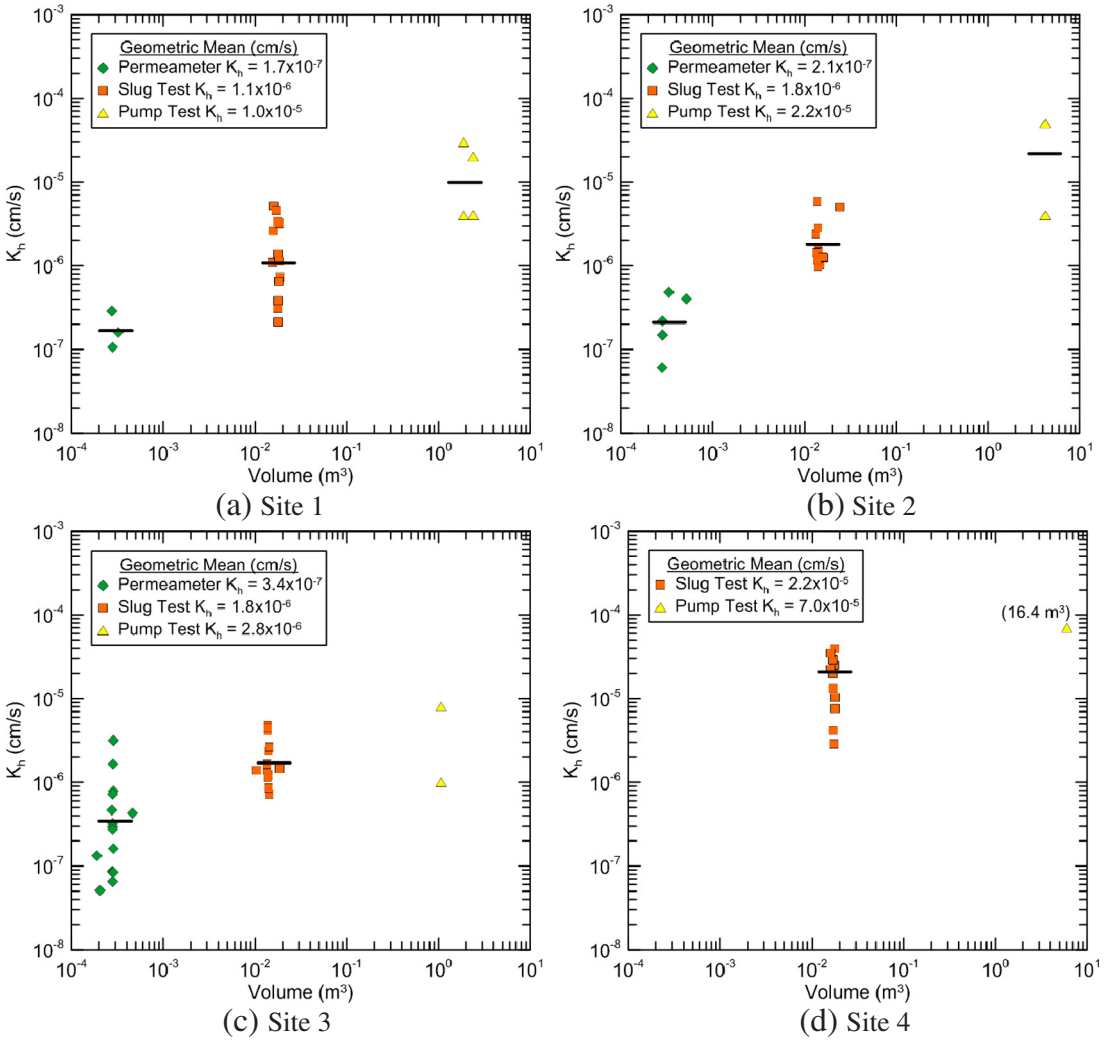

Fig. 11. Summary of scale effect on K_h results from laboratory experiments and field tests and corresponding geometric mean (solid line): (a) Site 1(b), Site 2, (c) Site 3, and (d) Site 4.

The significant range of permeameter K_h values at Site 3 also shows the influence of organics and macroflow paths. Although only one pump test was successfully performed at Site 4, Fig. 11(d) shows that the slug tests measure within the same magnitude of K_h. The compatibility between these two methods at Site 4 can be attributed to the high void ratio found in the decomposing vegetation and organics, which results in a higher K_h value and less scale effect.

A comparison of the three test methods shows the data are overlapping, which may question the effect of sample volume. As a result, Fig. 12 also provides the 90% confidence interval for laboratory permeameter, field slug, and field pump tests. These intervals signify that there is a 90% probability that the true mean of K_h is within these error bars. The largest confidence interval is reported for the permeameter because of the wide range of K_h measurements, with the field slug tests showing a high level of stability around the geometric mean. The relatively high confidence interval for the field pump tests is likely a result of limited number of tests. Because the confidence intervals do not overlap between the three methods, the increase in geometric K_h across the range of sample volume is statistically significant and can be represented by the trend line in Fig. 12.

Fig. 12 shows a trend line that can be used to predict the pump test related K_h based on a field slug or laboratory permeameter tests in these organic clay layers. The trend line follows the geometric mean of each method, so the equation does not account for the variability, i.e., standard deviation, within each method. However, it quantifies the scale effect for input into subsurface contaminant migration and subsidence

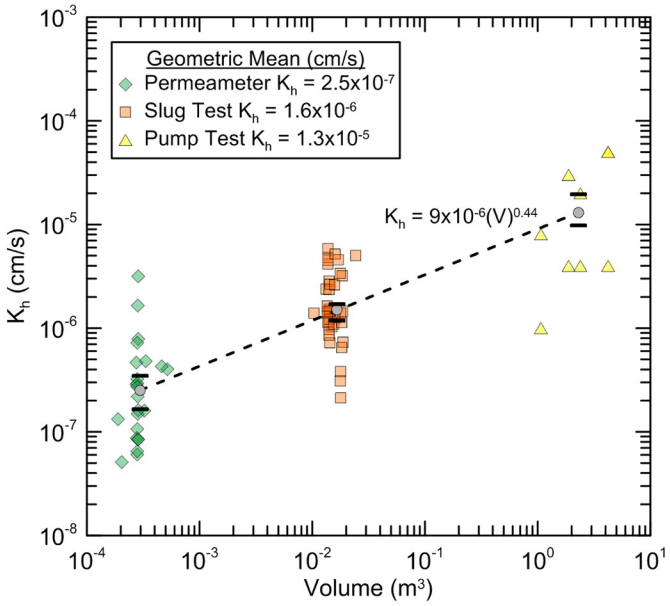

Fig. 12. Relationship of scale effect and K_h for Sites 1 through 3 showing values of geometric mean and 90% confidence interval of the geometric mean for laboratory permeameter, field slug, and field pump tests.

models. The scaling behavior can be described with the equation $K = c(V)^m$, where c is a parameter characteristic of geological medium that relates to geological variables, such as average pore size and interconnectivity in the porous media. The variable V is the volume of test material and m is the exponent of the relationship (slope of the line on a log-log plot). The value of the exponent depends on the type of flow present, with an exponent of about 0.5 characterizing homogeneous porous media (Schulze-Makuch et al., 1999) and values of 0.45 to 0.55 for unconsolidated sediments (Simpkins, 1989; Rodenback, 1988). The c values are a measure of the hydraulic conductivity at the scale of 1 m^3. Because this variable depends on soil and rock type, no general pattern typically appears in its distribution and values can range from c of 1.6×10^{-8} to 3.2×10^{-5} (Schulze-Makuch et al., 1999). Because Figs. 10 and 11 and Table 2 indicate that the geology between Sites 1 to 3 is similar, Fig. 12 combines all K_h data to develop a trend for volume of tested material and in situ K_h for the organic clay layers along the IHNC floodwall. This trend line in Fig. 12 consists of a c value of 9×10^{-6} and m exponent of 0.44. Based on Fig. 12, the geometric mean obtained from a laboratory permeameter test is about 52 times lower than the geometric mean of the field pump tests. The flow (Q) through an organic clay layer is equal to the area (A), hydraulic gradient (i), and hydraulic conductivity (K_h). For example, a 1 m thick clay layer with an assumed area of 10,000 m^2 and constant hydraulic gradient of 0.3 results in flow rates from 2.2 m^3/day to 112 m^3/day because of the scale effect in measuring hydraulic conductivity. As a result, laboratory permeameter tests can under predict fluid flow through the organic clay layers along the IHNC.

5.2. Uncertainty of hydraulic conductivity and compressibility

The multitude of tests used herein illustrates the variability in hydraulic conductivity and compressibility for the IHNC organic clays, which is important for performing reliability analyses and quantifying the uncertainty in contaminant migration, seepage, consolidation, and stability analyses. Fig. 13 shows the cumulative distribution of K_v and K_h obtained from permeameter tests and the slug test K_h. The K_v and K_h permeameter values in Fig. 13 follow a similar distribution, with K_h slightly higher than K_v for frequencies less than 0.65. The geometric means for both K are about 2×10^{-7} cm/s and the anisotropy ratio of the organic clay estimated at the geometric mean is about 1.2, which indicates the upper and lower organic clays along the IHNC are a homogeneous deposit (Terzaghi et al., 1996; Leroueil et al., 1992). The cumulative frequency for the permeameter and slug tests increases linearly between 0.1 and 0.9 in Fig. 13. This trend indicates that 80% of the data is explained in a narrow range of hydraulic conductivity. For example, the permeameter K_v and K_h occur between 4×10^{-8} and 1×10^{-6} cm/s. Similarly, the field slug test K_h distribution corresponds to a K_h of 4×10^{-7} to 6.3×10^{-6} cm/s. The field pump test trend in Fig. 13 represents the range of K_h obtained from the field tests in Sites 1 through 3. The overlap between the pump tests, permeameter, and slug tests provides an indication of the ability of each test to capture the in situ K_h. For example, 20% of the slug test K_h values are greater than the lower bound field K_h, while the maximum permeameter tests did not capture the scale-dependency in the field pump tests.

The consolidation tests performed as part of the site investigation provide a comparison between permeameter K_v and field pump test m_v. In total, forty-six (46) 1-D consolidation tests were compiled from incremental load and constant rate of strain tests to develop the

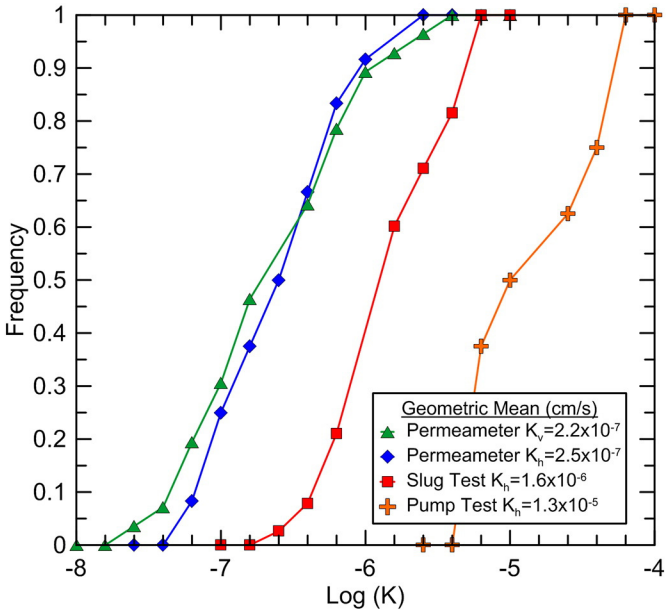

Fig. 13. Cumulative distribution of vertical and horizontal K and various test methods.

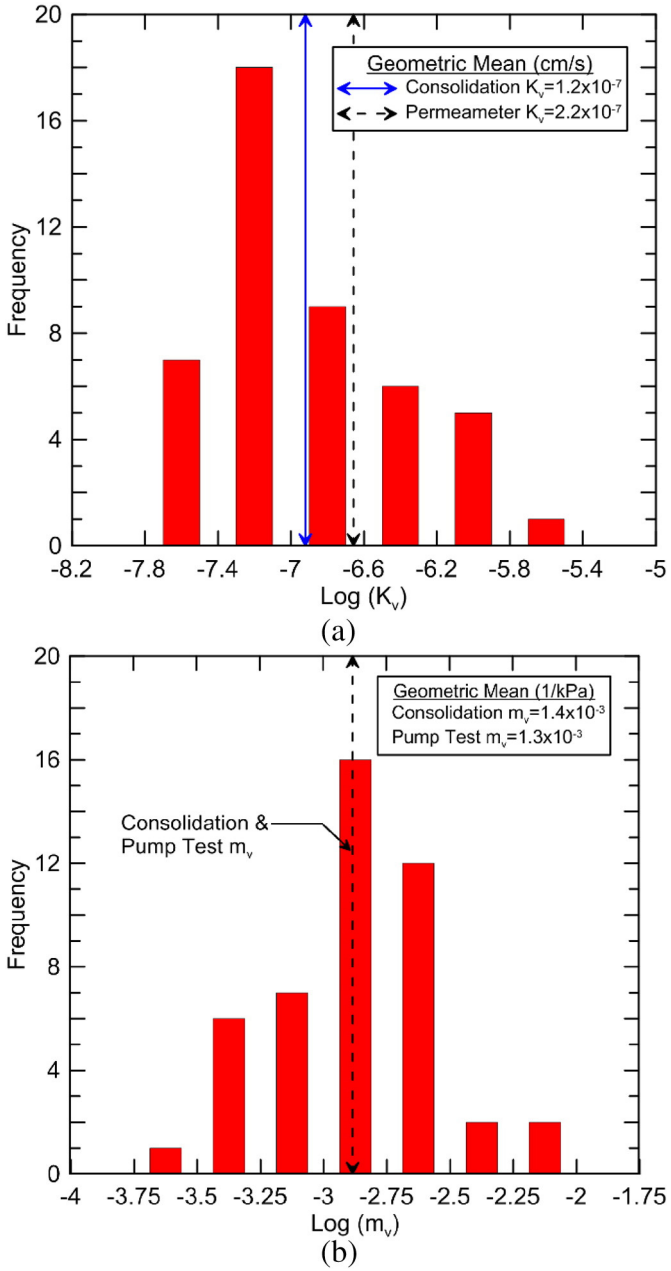

Fig. 14. Histograms developed from 1-D consolidation tests for: (a) K_v and (b) m_v.

histograms in Fig. 14. Both parameters were evaluated at the in situ overburden stress. The distribution of K_v and m_v in Fig. 14(a) and (b) suggests a lognormal distribution for both parameters. However, Fig. 14(a) shows a significant tail towards higher K_v values, which may indicate high organic content in the sample. The geometric mean of K_v from 1-D consolidometers is 1.2×10^{-7} cm/s, which is in agreement with the laboratory permeameter K_v of 2.2×10^{-7} cm/s. In Fig. 14(b), the geometric means of m_v for consolidation and field pump tests are 1.4×10^{-3} and 1.3×10^{-3} kPa^{-1}, respectively.

The field m_v was evaluated using the storativity ($S = S_s b$) obtained from inverse analyses of field pump tests and aquifer layer thickness (b) to determine the specific storage (S_s). Specific storage as a function of total porosity (n_t), soil compressibility (m_v), and water compressibility (β), i.e., $S_s = \gamma_w(m_v + n_t\beta)$. In application to soft organic soils, the compressibility of water (4.6×10^{-8} kPa^{-1}) is several orders of magnitude lower than soil (~10^{-3} kPa^{-1}). This causes the specific storage to reduce to $S_s = \gamma_w m_v$, permitting an estimate of m_v from field pump tests. It is evident from Fig. 14(b) that the field and laboratory compressibility values are in agreement, so a 1-D consolidation test is capable of estimating the field compressibility for transient seepage analyses involving these organic clay layers.

To quantify the variability of hydraulic conductivity (K) and m_v, Table 3 presents the COV for each test method. The COV is computed as the ratio of standard deviation to geometric mean. The COV of K_v is about 0.54 and 0.64 for laboratory 1-D consolidation and permeameter tests, respectively, which is slightly lower than the 0.68 to 0.90 as reported in Duncan (2000) and Harr (1987). The COV for K_h varies from 0.35 to 0.59, with the slug tests supplying the lower bound COV. The permeameter tests likely yield a relatively higher COV value because of the inclusion of organic pieces in the soil matrix, resulting in K_h varying more than the field slug test measurements. A lower COV was estimated for the permeameter K_h compared to the corresponding K_v. A possible factor for the increased variability in K_v is the orientation of the organics acting as preferential flow paths. The COV values for m_v show that the 1-D consolidation tests are lower than the field pump test. This difference may be attributed to the specimens prepared for consolidation tests that are trimmed to limit inclusion of organic roots or stems, i.e., a homogenous sample is tested instead of a field representative sample (Olson and Daniel, 1981). In summary, mean and COV values in Table 3 can be used for future uncertainty analysis for consolidation and contaminant flow problems in these organic clays.

6. Summary

This paper describes an extensive site investigation performed at the IHNC in New Orleans, Louisiana to understand the scale-effect on hydraulic conductivity and compressibility of the underlying organic clays. The laboratory experiments, including 1-D consolidation and flexible wall permeameter, were supplemented with in situ CPTu dissipation, field slug, and field pump tests. Test procedures and analyses are described herein for the field pump tests because these tests are time consuming and expensive and not typically performed in organic clays. The site investigation found that the geology and geotechnical properties along Sites 1 through 3 are spatially similar. A summary of the results from these analyses is:

Table 3
Values of COV for K and m_v from Sites 1 to 3.

Parameter	Test	Geometric Mean	COV
K_v (cm/s)	1-D consolidation	1.2×10^{-7}	0.54
	Permeameter	2.2×10^{-7}	0.64
	Permeameter	2.5×10^{-7}	0.46
K_h (cm/s)	Slug	1.6×10^{-6}	0.35
	Pump	1.3×10^{-5}	0.59
m_v (kPa^{-1})	1-D consolidation	1.4×10^{-3}	0.34
	Pump	1.3×10^{-3}	0.73

- The organic clays along the IHNC at the LNW show a scale effect of an order of magnitude when increasing the specimen volume from laboratory permeameter to field pumps tests. This scale effect is captured by the equation $K_h = 9 \times 10^{-6}(V)^{0.44}$ where V is the volume of material tested, which can be used to estimate field K_h for preliminary geotechnical and geoenvironmental analyses in these organic clays.
- The cumulative distribution of K_v and K_h values obtained from permeameter tests shows that the lower organic clay layer is mostly homogenous with an anisotropy ratio of about 1.2. The distribution of K and m_v values, including the consolidation tests, can be approximated by lognormal. The COV for K and m_v is provided and can be used for reliability analyses.
- The site investigation shows that field tests are necessary to capture the macro level flow and field hydraulic conductivity of these organic clays. However, a comparison of soil compressibility from field and 1-D consolidation tests suggests that a 1-D consolidation test can be used to predict the field value of m_v for transient seepage problems. The values of K_h and m_v for these organic clays are applicable to contaminant transport, shallow groundwater flow, time-dependent consolidation, transient seepage, and shear strength for stability of foundations and embankments.

Acknowledgments

The contents and views in this paper are those of the authors and do not necessarily reflect those of any dam or reservoir owner/operator, consultant, regulatory agency or personnel, or anyone else knowledgeable about the case study referenced. In particular, the contents of this paper/publication are the personal opinions of the author(s) and may not reflect the opinions, conclusions, policies or procedures of the U.S. Army Corps of Engineers or the U.S. Department of Justice.

Appendix A. Supplementary data

Supplementary data to this article can be found online at http://dx.doi.org/10.1016/j.enggeo.2017.01.015.

References

Agarwal, R.G., 1980. A new method to account for producing time effects when drawdown type curves are used to analyze pressure buildup and other test data. 55th SPE Annual Technical Conference and Exhibition. Dallas, Society of Petroleum Engineers.
ASTM International, 2004a. D5092. Standard Practice for Design and Installation of Groundwater Monitoring Wells, West Conshohocken, Pa.
ASTM International, 2004b. D6724. Standard Guide for Installation of Direct Push Groundwater Monitoring Wells, West Conshohocken, Pa.
ASTM International, 2006. D7242/D7242M. Standard Practice for Field Pneumatic Slug (Instantaneous Change in Head) Tests to Determine Hydraulic Properties of Aquifers with Direct Push Groundwater Samplers, West Conshohocken, Pa.
ASTM International, 2010a. D2216. Standard Test Methods for Laboratory Determination of Water (Moisture) Content of Soil and Rock by Mass, West Conshohocken, Pa.
ASTM International, 2010b. D5084. Standard Test Methods for Measurement of Hydraulic Conductivity of Saturated Porous Materials Using a Flexible Wall Permeameter, West Conshohocken, Pa.
ASTM International, 2011a. D2435/D2435M. Standard Test Methods for One-Dimensional Consolidation Properties of Soils Using Incremental Loading, West Conshohocken, Pa.
ASTM International, 2011b. D2487. Standard Practice for Classification of Soils for Engineering Purposes (Unified Soil Classification System), West Conshohocken, Pa.
ASTM International, 2012. D4186/D4186M. Standard Test Method for One-Dimensional Consolidation Properties of Saturated Cohesive Soils Using Controlled-Strain Loading, West Conshohocken, Pa.
ASTM International, 2013. D4427. Standard Classification of Peat Samples by Laboratory Testing, West Conshohocken, Pa.
ASTM International, 2014a. D2974. Standard Test Methods for Moisture, Ash, and Organic Matter of Peat and Other Organic Soils, West Conshohocken, Pa.
ASTM International, 2014b. D4050. Standard Test Method for (Field Procedure) for Withdrawal and Injection Well Testing for Determining Hydraulic Properties of Aquifer Systems, West Conshohocken, Pa.
ASTM International, 2014c. F480. Standard Specification for Thermoplastic Well Casing Pipe and Couplings Made in Standard Dimension Ratios (SDR), SCH 40 and SCH 80, West Conshohocken, Pa.
ASTM International, 2015a. D1587/D1587M. Standard Practice for Thin-Walled Tube Sampling of Fine-Grained Soils for Geotechnical Purposes, West Conshohocken, Pa.

ASTM International, 2015b. D4044/D4044M. Standard Test Method for (Field Procedure) for Instantaneous Change in Head (Slug) Tests for Determining Hydraulic Properties of Aquifers, West Conshohocken, Pa.
Benson, C.H., Zhai, H., Wang, X., 1994. Estimating hydraulic conductivity of compacted clay liners. J Geotech Eng 120 (2), 366–387.
Bouwer, H., Rice, R.C., 1976. A slug test for determining hydraulic conductivity of unconfined aquifers with completely or partially penetrating wells. Water Resources Research 12, 423–428.
Bradbury, K.R., Muldoon, M.A., 1990. Long-term monitoring of groundwater quality in an area of fractured dolomite, minor karst, and thin soils. 1990 Annual Meeting. Geological Society of America, Dallas.
Burns, S.E., Mayne, P.W., 1998. Penetrometers for soil permeability and chemical detection. Georgia Institute of Technology Report GIT-CEEGEO-98-1.
Casagrande, A., Fadum, R.E., 1940. Notes on soil testing for engineering purposes. Harvard University Graduate School of Engineering Publication No. 8 (129 p).
Chapuis, R.P., 1990. Sand-bentonite liners: predicting permeability from laboratory tests. Can Geotech J 27 (1), 47–57.
Chapuis, R.P., 1998. Overdampled slug test in monitoring wells: review of interpretation methods with mathematical, physical, and numerical analysis of storativity influence. Can Geotech J 35, 697–719.
Chapuis, R.P., 2004. Permeability tests in rigid-wall permeameters: determining the degree of saturation, its evolution and influence on test results. Can Geotech J 41 (5), 787–795.
Chapuis, R.P., 2012. Predicting the saturated hydraulic conductivity of soils: a review. Bull. Eng. Geol. Environ. 71, 401–434.
Chapuis, R.P., Chenaf, D., 2002. Slug tests in a confinded aquifer: experimental results in a large soil tank and numerical modeling. Can Geotech J 39, 14–21.
Chapuis, R.P., Dallaire, V., Marcotte, D., Chouteau, M., Acevedo, N., Gagnon, F., 2005. Evaluating the hydraulic conductivity at three different scales within an unconfined sand aquifer at Lachenaie, Quebec. Can Geotech J 42, 1212–1220.
Cooper, H.H., Jacob, C.E., 1946. A generalized graphical method for evaluating formation constants and summarizing well field history. Am Geophys Union Trans 27, 526–534.
Duffield, G.M., 2007. AQTESOLV for Windows Version 4.5 User's Guide. HydroSOLVE, Inc., Reston, Va.
Dunbar, J.B., Britsch, L.D., 2008. Geology of the New Orleans Area and the Canal Levee Failures. Journal of Geotechnical and Geoenvironmental Engineering 134:566–582. http://dx.doi.org/10.1061/(asce)1090-0241(2008)134:5(566).
Duncan, J.M., 2000. Factors of safety and reliability in geotechnical engineerign. J Geotech Geoenviron Eng 126, 307–316.
Fetter, C.W., 1988. Applied Hydrogeology. 2 ed. Merrill Publishing Company, Inc., Princeton, N.C.
Flawn, P.T., Turk, L.J., Leach, C.H., 1970. Geological Considerations in Disposal of Solid Municipal Wastes in Texas. The University of Texas at Austin, Bureau of Economic Geology.
Freeze, R.A., Cherry, J.A., 1979. Groundwater. first ed. Prentice Hall, Englewood Cliffs, N.J.
Hanor, J.S., 1993. Effective hydraulic conductivity of fractured clay beds at a hazardous waste landfill, Louisiana Gulf Coast. Water Resources Research 29:3691–3698. http://dx.doi.org/10.1029/93wr01913.
Hantush, M.S., 1959. Nonsteady flow to flowing wells in leaky aquifers. Journal of Geophysical Research 64:1043–1052. http://dx.doi.org/10.1029/JZ064i008p01043.
Harr, M.E., 1987. Reliability-based design in civil engineering. McGraw-Hill, New York.
Hvorslev, M.J., 1951. Time lag and soil-permeability in ground-water observations. Waterways Experiment Station Report Bulletin No. 36.
Jones, L., 1993. A comparison of pumping and slug tests for estimating the hydraulic conductivity of unweathered Wisconsian age till in Iowa. Ground Water 31:896–904. http://dx.doi.org/10.1111/j.1745-6584.1993.tb00862.x.
Kruseman, G.P., de Ridder, N.A., 1990. Analysis and Evaluation of Pumping Test Data. second ed. International Institute for Land Reclamation and Improvement, Wageningen, The Netherlands.
Leroueil, S., Leart, P., Hight, D.W., Powell, J.J.M., 1992. Géotechnique 42 (2), 275–288.
McWhorter, D.B., Sunada, D.K., 1977. Ground-water Hydrology and Hydraulics. Water Resources Publications, LLC, Highlands Ranch, Calif.
Moench, A.F., 1985. Transient flow to a large-diameter well in an aquifer with storative semiconfining layers. Water Resources Research 21:1121–1131. http://dx.doi.org/10.1029/WR021i008p01121.
Neuman, S.P., 1974. Effect of partial penetration on flow in unconfined aquifers considering delayed gravity response. Water Resources Research 10:303–312. http://dx.doi.org/10.1029/WR010i002p00303.
Neuzil, C.E., 1986. Groundwater flow in low-permeability environments. Water Resources Research 22:1163–1195. http://dx.doi.org/10.1029/WR022i008p01163.
Olson, R.E., Daniel, D.E., 1981. Measurement of the hydraulic conductivity of fine-grained soils. In: Zimmie, T.F., Riggs, CO. (Eds.), Permeability and Groundwater Contaminant Transport. ASTM Spec. Tech. Publ. 746, pp. 18–64.
Parez, L., Fauriel, R., 1988. Advantages from piezocone application to in-situ tests. Révue Française de Géotechnique 44, 13–27.
Peyton, G.R., Gibb, J.P., LeFaivre, M.H., Ritchey, J.D., Burch, S.L., Barcelona, M.J., 1986. Effective porosity of geologic materials. 12th Ann. Res. Symp. U.S. Environmental Protection Agency, Cincinatti, Ohio, pp. 21–28.
Ratnam, S., Soga, K., Whittle, R.W., 2005. A field permeability measurement technique using a conventional pressuremeter. Géotechnique 55, 527–537.
Robertson, P.K., Sully, J.P., Woeller, D.J., Lunne, T., Powell, J.J.M., Gillespie, D.G., 1992. Estimating coefficient of consolidation from piezocone tests. Canadian Geotechnical Journal 29:539–550. http://dx.doi.org/10.1139/t92-061.
Rodenback, S.A., 1988. Merging Pleistocene lithostratigraphy with geotechnical and hydrogeologic data—examples from eastern Wisconsin. M.S., University of Wisconsin-Madison.
Rovey, C.W., Cherkauer, D.S., 1995. Scale dependency of hydraulic conductivity measurements. Ground Water 33, 769–780.
Schmertmann, J.H., 1978. Guidelines for Cone Penetration Tests Performance and Design. U.S. Federal Highways Administration, Washington.
Schulze-Makuch, D., Carlson, D.A., Cherkauer, D.S., Malik, P., 1999. Scale dependency of hydraulic conductivity in heterogeneous media. Ground Water 37:904–919. http://dx.doi.org/10.1111/j.1745-6584.1999.tb01190.x.
Simpkins, W.W., 1989. Unusual involutions in diamicton of the Pleistocene Oak Creek Formation: glacial deformation or sediment loading? 1989 Annual Meeting. Geological Society of America, St. Louis
Smith, C.G., Kazmann, R.G., 1978. Subsidence in the capital area ground water conservation district — an update. Capital Area Ground Water Conservation Commission Report Bulletin No. 3.
Stark, T.D., Jafari, N.H., 2015. Ruling on IHNC floodwall failures during Hurricane Katrina. J. of Legal Affairs and Dispute Resolution in Engineering Construction 7 (3), 1–11.
Tartakovsky, G.D., Neuman, S.P., 2007. Three-dimensional saturated-unsaturated flow with axial symmetry to a partially penetrating well in a compressible unconfined aquifer. Water Resources Research:43 http://dx.doi.org/10.1029/2006wr005153.
Tavenas, F., Jean, P., Leblond, P., Leroueil, S., 1983. The permeability of natural soft clays. Part I: methods of laboratory measurement. Can Geotech J 20 (4), 629–644.
Taylor, D.W., 1942. Research on Consolidation of Clays. Serial No. 82. Department of Civil and Sanitary Engineering, Massachusetts Institute of Technology, Cambridge, Mass.
Taylor, R.J., 1993. Superfunds Site of Harris County, Texas. Houston Geological Society, Houston.
Terzaghi, K., Peck, P.B., Mesri, G., 1996. Soil Mechanics in Engineering Practice. John Wiley & Sons, Inc., New York.
Theis, C.V., 1935. The relation between the lowering of the piezometric surface and the rate and duration of discharge of a well using groundwater storage. Am Geophys Union Trans 16, 519–524.